

2

REPORT DO			READ INSTRUCTIONS BEFORE COMPLETING FORM
1. REPORT NUMBER	3. RECIPIENT'S CATALOG NUMBER		
# 16			
4. TITLE (and Subtitle)		5. TYPE OF REPORT & PERIOD COVERED	
Effect of TCP Doping on the Remnant Polarization in Uniaxially Oriented Poly(vinylidene fluoride) Films		Technical Report	
7. AUTHOR(s)		6. PERFORMING ORG. REPORT NUMBER	
Y. Takase, J.I. Scheinbeim and B.A. Newman			
9. PERFORMING ORGANIZATION NAME AND ADDRESS		8. CONTRACT OR GRANT NUMBER(s)	
Rutgers, The State University of New Jersey College of Engineering, P.O. Box 909 Piscataway, NJ 08855-0909		N00014-88-K-0122	
11. CONTROLLING OFFICE NAME AND ADDRESS		12. REPORT DATE	
Dr. Joanne Milliken Office of Naval Research Arlington, VA 22217		May 1991	
14. MONITORING AGENCY NAME & ADDRESS (if different from Controlling Office)		13. NUMBER OF PAGES	
		28	
		15. SECURITY CLASS. (of this report)	
		Unclassified	
		15a. DECLASSIFICATION/DOWNGRADING SCHEDULE	
16. DISTRIBUTION STATEMENT (of this Report)			
Approved for public release; distribution unlimited. Reproduction in whole or in part is permitted for any purpose of the United States Government			
17. DISTRIBUTION STATEMENT (of the abstract entered in Block 20, if different from Report)			
18. SUPPLEMENTARY NOTES			
Published, Macromolecules			
19. KEY WORDS (Continue on reverse side if necessary and identify by block number)			
20. ABSTRACT (Continue on reverse side if necessary and identify by block number)			
Uniaxially stretched films of poly(vinylidene fluoride) were doped (1 wt. %) with plasticizer, tricresyl phosphate (TCP). This slight doping with TCP was found to enhance the amount of remnant polarization in the region of low poling fields (e.g., from 1 to 6 mC/m ² under E _p = 60 MV/m at 20°C) and high poling fields (e.g., from 57 to 66 mC/m ² under E _p = 200 MV/m at 20°C). The pyroelectric coefficient has shown that the doping enhances a quite stable (up to about 140°C) remnant polarization after high field poling (e.g., from 10.2 to 12.5 μC/m ² /K under E _p = 200 MV/m at 20°C). This suggestive of a field induced increase in crystallinity. In addition, the switching of quasi-stable dipoles (those which randomize in the			


91-01964

OVER

90 - 140°C range) takes place at much lower electric fields than in undoped films. The present data suggest that a small amount of dopant in the noncrystalline regions greatly enhances ferroelectric dipole switching, possibly by acting in the interfacial zone between crystalline and amorphous regions.

Unclassified

OFFICE OF NAVAL RESEARCH

Contract N00014-88-K-0122

Technical Report No. 16

Effect of TCP Doping on the Remnant Polarization in
Uniaxially Oriented Poly(vinylidene fluoride) Films

by

Y. Takase, J.I. Scheinbeim and B.A. Newman

Prepared for Publication in

Macromolecules

Department of Mechanics and Materials Science
College of Engineering
Rutgers University
Piscataway, NJ 08855-0909

May 1991

Reproduction in whole or in part is permitted for any purpose of the
United States Government

This document has been approved for public release and sale; its distribution
is unlimited

Effect of TCP Doping on the Remnant Polarization
in Uniaxially Oriented Poly(Vinylidene Fluoride) Films

Y. Takase,* J. I. Scheinbeim, and B. A. Newman

Department of Mechanics and Materials Science, College
of Engineering, Rutgers University, Piscataway, New
Jersey 08854

ABSTRACT: Uniaxially stretched films of poly(vinylidene fluoride) were doped (1 wt. %) with plasticizer, tricresyl phosphate (TCP). This slight doping with TCP was found to enhance the amount of remnant polarization in the region of low poling fields (e. g. from 1 to 6 mC/m^2 under $E_p = 60 \text{ MV}/\text{m}$ at 20°C) and high poling fields (e. g. from 57 to 66 mC/m^2 under $E_p = 200 \text{ MV}/\text{m}$ at 20°C). The pyroelectric coefficient has shown that the doping enhances a quite stable (up to about 140°C) remnant polarization after high field poling (e. g. from 10.2 to 12.5 $\mu\text{C}/\text{m}^2/\text{K}$ under $E_p = 200 \text{ MV}/\text{m}$ at 20°C). This is suggestive of a field induced increase in crystallinity. In addition, the switching of quasi-stable dipoles (those which randomize in the $90 - 140^\circ\text{C}$ range) takes place at much lower electric fields than in undoped films. The present data suggest that a small amount of dopant in the noncrystalline regions greatly enhances ferroelectric dipole switching, possibly by acting in the interfacial zone between crystalline and amorphous regions.

Introduction

Plasticized polymers, such as the poly(vinyl chloride)-tricresyl phosphate (PVC-TCP) system, offer significant advantages in their physical properties such as toughness, flexibility, oil-resistance, and non-flammability as well as high electrical resistance when compared to unplasticized polymers.

Recently, it was found in our laboratories that the addition of plasticizer to poly(vinylidene fluoride) (PVF_2) films has a significant influence on their piezoelectric and pyroelectric properties. Sen et al.¹ prepared two different types of samples to examine the effects of TCP doping. One type of sample was unoriented phase II PVF_2 film which was prepared by melt crystallization. The other type of sample was oriented phase I PVF_2 film which was obtained from the phase II film by uniaxial stretching at 54°C. For doping, the film was immersed in TCP at elevated temperatures.

In the case of the initially unoriented phase II films, the piezoelectric and pyroelectric coefficients of the doped films showed significantly improved values compared to those of the undoped films when poled under identical conditions. The results of X-ray diffraction studies of both types of samples showed that for the doped films, the phase transformation from the nonpolar phase II crystal form to the polar phase I crystal form had taken place at much lower poling fields than for undoped films.

In the case of the uniaxially oriented phase I films, doping also led to a large increase in piezoelectric and pyroelectric response.

Although X-ray diffraction data of the doped films have suggested that some preferential positioning of the dopant at the crystallite boundaries may occur, with no evidence of diffusion of the dopant into the crystalline regions, additional studies are required to gain some understanding of the mechanisms involved.

PVF₂ is a semicrystalline polymer and its crystallinity is usually around 50 %²⁻⁵ (recently, perdeuteriated PVF₂ films were found to have much higher crystallinity⁶). Since there was no indication (from X-ray diffraction studies) of the plasticizer diffusing into the crystalline regions,¹ most of the plasticizer must be in solution outside the crystalline regions. The effect of the plasticizer on the bulk properties of PVF₂ film may therefore be understood in terms of the activity of the dopant on a heterogeneous system which consists of crystalline regions and plasticized amorphous regions and their interface zones.

One possible way to identify the role of plasticizer in this complicated system is to only slightly dope the sample to ensure that the plasticizer does not change too many physical parameters simultaneously (i. e. modulus, dielectric constant, thermal expansion) and to detect any significant effects by some set of sensitive measurements.

A recent study carried out by Takase et al.⁷ on the polarization reversal characteristics of PVF₂ provides suggestions concerning such measurements. They used a γ -ray irradiation technique in order to identify the different roles of dipoles whose arrangement covers a range from an amorphous state to a well ordered crystalline state. This study was based on the

assumption that molecular chains within the crystals are less affected by γ -ray irradiation than chains in the amorphous regions.⁸ It was found that the effect of irradiation was most pronounced during the initial stage of the polarization reversal process i. e. on the nucleation stage.⁷ A very likely place for the nucleation process to occur is the interfacial zone between the crystalline and amorphous regions. If we add a small amount of dopant to the PVF₂ film, we should observe an effect which may be a counterpart to the γ -ray irradiation effect, i. e. something which appears not to alter the crystalline regions while slightly altering the amorphous regions and the interface zones.

In the present study, we prepared doped samples by the same immersion method used by Sen et al.¹ but we changed some sample and measurement conditions. We used the same stretched films previously used by several other researchers for polarization reversal measurements,^{7,9-12} to examine consistency with previous data. We limited the temperature and time of the immersion process to much less than those used by Sen et al.,¹ so as to minimize change in the physical condition of the crystalline regions and we then examined the change in remnant polarization, P_r , which is the most fundamental parameter related to piezoelectric and pyroelectric properties.

As a result, we hoped to show some marked effect of the dopant on the electric displacement, D , on the depolarization current (DPC) and on the pyroelectric coefficient, p_y , of the PVF₂ films. Based on detailed data obtained under various poling conditions, the role of the dopant in enhancing the remnant

polarization was examined.

Experimental Section

Samples used in this study were 7- μm -thick uniaxially oriented PVF₂ films (KF1000) supplied by Kureha Chemical Industry, Co., Ltd. These films are the same as those used in several previous studies^{7,9-12} and, in addition, 97 % of the crystalline material is in the phase I form.¹⁰ Annealed samples were prepared by heat treatment in vacuum at 120°C for 2 hours. During annealing, the film was mechanically clamped to prevent shrinkage.

Doped samples were prepared by immersing the annealed films in tricresyl phosphate at 100°C for 4 hours. The temperature and immersion time were much less than those used (130 °C for 24 hours) by Sen et al.¹ The dopant content was only about 1 % by weight. Hereafter, undoped sample refers to the as annealed undoped film.

Gold electrodes, each about 3 x 10 mm² in area, were deposited on opposing surfaces of the films by vacuum evaporation. All measurements, except X-ray measurements, were carried out by placing the sample in an electrically shielded copper cell which was equipped with a heater and temperature sensor.

X-ray diffraction profiles were obtained at room temperature with a Philips XRG 3100 X-ray generator. CuK α radiation filtered with a Ni foil was used.

The D - E hysteresis characteristics were measured at 20°C

using a high voltage power supply and a picoammeter (Keithley 485) connected in series with the sample. The period of the triangular shaped high voltage wave was 1000 s.

The pyroelectric coefficient and depolarization current were obtained from samples poled by applying a step voltage pulse of 1 min width at room temperature, then the thermally stimulated current was measured by the picoammeter as the sample was subjected to heating and cooling cycles at a rate of 2 °C/min.

Operation of various functions in the system were consigned to a microcomputer (IBM-XT) which also performed the task of data processing.

Results

1. X-ray Diffraction Profiles. The diffractometer scans for the as-received, annealed and doped samples in reflection mode are shown in Figure 1. Table I shows the 2θ values and half widths, $\beta_{1/2}$, for the composite (110)(200) reflection of the phase I crystals in the above three samples. It is seen that the annealed sample exhibits a larger 2θ value, a smaller half width and a larger peak height than the as-received samples, indicating a decrease in interplaner separation caused by better packing and increased perfection and size of the crystallites.

Figure 1

Table I

The doped sample does not exhibit significant change in 2θ value and half width from those of the annealed sample, although there may be a slight additional annealing effect caused by the immersion in TCP at 100 °C for 4 hours. The doping process did not cause the phase I crystalline material to transform to other

phases. Differing from the results of Sen et al.¹, the major shift in 2θ value was brought about not by doping and poling but by heat treatment alone, and the doping did not broaden the half width. Therefore, as expected, the low level of dopant did not appear to diffuse into or significantly affect the structure of the crystalline regions, even with regard to the poling field induced 2θ changes observed by Sen et al. at higher (5 %) dopant levels.

Fig.2(a)
Fig.2(b)

2. D - E Hysteresis Characteristics. Figures 2 (a) and (b) show current density, J , and electric displacement, D , respectively, as a function of electric field when the samples are subjected to triangular electric field pulses with maximum fields of 60, 120 and 200 MV/m. The dotted lines represent data for the doped samples and the continuous lines for the undoped samples.

Significant differences between the data of the doped and undoped samples are observed. The doped samples show a well defined peak on the $J - E$ curves (Figure 2 (a)), even if the peak value of E , E_p , is comparatively low; around 60 MV/m. The $D - E$ hysteresis curve (Figure 2 (b)), corresponding to the $J - E$ curve for $E_p = 60$ MV/m, exhibits a certain amount of remnant polarization (11 mC/m^2). On the other hand, the undoped sample does not show the peak and exhibits a propeller like $D - E$ hysteresis curve (Figure 2 (b)), which indicates that a small number of dipoles orient under the application of an electric field of 60 MV/m but their orientation is not stable enough to exhibit remnant polarization. This data indicates that

ferroelectric dipole orientation is significantly enhanced by the presence of a small amount of TCP outside the crystalline regions of the film.

When the amplitude of the field is 120 MV/m, the doped sample shows a sharp peak on the J - E curve (Figure 2 (a)). Under this field, the undoped sample shows a broad peak on the J - E curve, indicating a polarization reversal originating from some initial field induced (crystal) dipole orientation. Both samples exhibit almost the same amount of remnant polarization, as is indicated on the D - E hysteresis curves (Figure 2 (b)).

When the field amplitude becomes as high as 200 MV/m, each sample shows a sharp peak on the J - E curve (Figure 2 (a)). The value of remnant polarization of the undoped sample, about 57 mC/m^2 as indicated on the D - E curve (Figure 2 (b)), is known to be almost a saturated value at 20°C .¹¹ The doped sample, however, exhibits a value of about 66 mC/m^2 (average value of $+P_r$ and $-P_r$ in Figure 2 (b)) which is 16 % larger than that of the undoped sample. The J - E curve (Figure 2 (a)) indicates that the increase in P_r of the doped sample is caused by an increase in the current component of polarization reversal in the field region higher than the coercive field. It is surprising that only 1 wt. % of dopant enhances the remnant polarization by 16 % in the high poling field region as well as the enormous enhancement of P_r in the low poling field region.

3. Depolarization Current. The D - E hysteresis characteristics show the essential features of ferroelectric polarization reversal and give the value of remnant polarization;

however, they do not reveal sufficient information about the polarization reversal mechanism, especially of semicrystalline polymers. In such polymers, not only does the dipole motion within the crystallites differ from that outside but also differs among crystallites; several physical parameters depend on crystallite size.¹³⁻¹⁵ The depolarization current of ferroelectric materials yields information about the thermal stability of the oriented dipoles which reflects their environment in the amorphous regions, the microdomains in small crystallites, and domains in the "usual" crystallites.

The depolarization current densities of the doped and undoped samples are shown in Figures 3 (a) and (b), respectively. Curves (1) - (4) represent the current density for samples poled by a 1 min step pulse of 20, 60, 120, and 200 MV/m field strength, respectively, and curve (5) poled by sequential step pulses of 200 MV/m strength applied in opposite directions. Both samples exhibit one or two current density peaks over the temperature measurement region. A low temperature peak appears in the temperature region 30 - 40°C and the peak shifts slightly to the high temperature side as the poling field increases. A high temperature peak appears around 90°C when the poling field is 20 and 60 MV/m. This peak shifts rapidly to the high temperature side as the poling field increases.

Fig. 3(a)
Fig. 3(b)

The marked effect of dopant is also present in the depolarization current. When the poling field is comparatively low, the doped sample shows much higher first and second peaks than those of the undoped sample. The increase in the second peak

is prominent after doping; the height is five times larger than that of the undoped sample at $E_p = 60$ MV/m (see curve (2)). When the field is as high as 200 MV/m, the second peak shifts to a temperature region higher than 140°C and only the broad tail of it can be seen for the doped sample (see curve (4)). After applying a second poling field in the reverse direction, the first peak height (of curve (5)) increases to twice the size of that (of curve (4)) of the sample poled using a single step pulse and the height difference of the first peak between the two types of samples is reversed (see curve (5) in Figures 3 (a) and (b)).

Figure 4 presents the depolarization current vs temperature data which looks at the effects of the polarization reversal process for both the doped (dotted lines) and the undoped (continuous lines) samples. Curve (1) represents characteristics of the sample poled under $E_p = +200$ MV/m, and curve (2) for the sample poled under $E_p = +200$ MV/m and then $E_p = -200$ MV/m. These two curves are essentially symmetric with respect to the temperature axis, indicating complete polarization reversal.

Curves (3) and (4) represent characteristics of the samples which are subjected to the poling sequence $+200$ MV/m, -200 MV/m, followed by polarization reversal produced by applying field of $E_p = +20$ and $+40$ MV/m, respectively. This was done to gain some further insight into the polarization reversal process. This will be discussed later.

4. Pyroelectric Coefficient. PVF_2 does not show a ferroelectric to paraelectric phase transition before melting occurs; therefore, it is impossible to know the total remnant

Figure 4

polarization of the sample by simple integration of the depolarization current (DPC) unless the sample is taken to the melting point. However, we can estimate P_r from the pyroelectric coefficient, p_y , since it is proportional to the remnant polarization.¹⁶

Figures 5 (a) and (b) show the p_y vs T characteristics of the doped and the undoped samples, respectively. The value of p_y is calculated from the DPC on the cooling cycle after heating up to 140°C, so that p_y reflects only the high temperature stable remnant polarization. p_y is obtained from the relation:

$$p_{yi} = (J_i - J_{i-1})(t_i - t_{i-1}) / (T_i - T_{i-1}), \quad (1)$$

where J is the current density, t the time, T the temperature and the subscript i denotes the sampling number. Curves (1) - (9) represent data obtained under different poling conditions as follows; (1) - (5): a step pulse of +20, +80, +120, +160, and +200 MV/m, respectively, (6): sequential step pulses of +200, -200 and +200 MV/m, (7): a step pulse of +200 MV/m followed by -200 MV/m, (8): sequential step pulses of +200, -200 and +20 MV/m, and (9): sequential step pulses of +200, -200 and +40 MV/m.

When the poling field is 80 MV/m or lower, the value of p_y is essentially zero indicating complete decay of the remnant polarization after the process of heating up to 140°C. Therefore, integration of the depolarization current up to 140°C gives the remnant polarization; for example the integration of curve (2) in Figure 3 gives 6 mC/m² and 1 mC/m² under $E_p = 60$ MV/m for doped and undoped samples, respectively. These values are essentially consistent with the hysteresis data ($P_r = 11$ and 1 mC/m² shown in

Fig. 5(a)
Fig. 5(b)

Figure 2 (b)) since the DPC is measured sometime after poling and some of the unstable polarization has decayed. As the poling field increases up to 120 MV/m, the value of p_y slightly increases for both doped and undoped samples. This is consistent with the DPC data, since the tail of the second peak goes into the temperature region above 140°C (see Figure 3). The increase in poling field from 120 to 160 MV/m brings about a large increase in p_y , from -0.9 to -5.7 $\mu\text{C}/\text{m}^2/\text{K}$ at 40°C, for the doped sample and -0.9 to -4.5 $\mu\text{C}/\text{m}^2/\text{K}$ at 40°C for the as-annealed sample. This is indicative of a large enhancement of the stable remnant polarization which does not decay by heating up to 140°C. It is also clear that the stable remnant polarization increases when the sample is poled by a train of electric field step pulses applied in reversed directions. When the sample is poled in a reversed direction, the polarity of p_y reverses. The value of p_y of the doped samples after the reversal is 12.5 $\mu\text{C}/\text{m}^2/\text{K}$, which is larger by 22 % than the 10.2 $\mu\text{C}/\text{m}^2/\text{K}$ of the as-annealed samples. This is also quite consistent with the D - E hysteresis data (16 % increase in P_r as shown in Figure 2(b)).

Discussion

1. Dopant Effect in the Low Poling Field Region. When the samples are poled below about 80 MV/m, the dopant effect is the most prominent. The amount of P_r in the doped sample is several times larger than that of the undoped samples under identical poling conditions. The DPC measurements indicate that P_r originates from the orientation of thermally unstable dipoles

which totally randomize on heating up to 140 °C. The fact that this effect is strongest at low poling fields may indicate that the thermally unstable dipoles are located in an environment which is directly affected by the noncrystalline regions where the dopant exists.

2. Dopant Effect in the High Poling Field Region. A marked dopant effect is observed after polarization reversal. The thermally stable dipole orientation is significantly enhanced after repeated application of high reversed poling fields which may be interpreted as producing a certain amount of additional crystal growth at the interfacial zones. Even in undoped films, Takahashi and Odajima¹⁷ observed this type of crystal growth by X-ray measurements. As shown by our previous study,¹ field induced crystal growth is greatly enhanced in doped films. In the present study, this process is reflected in the J - E curve in Figure 2 (a), where the value of J for the doped sample, in the field region higher than the coercive field, significantly increases compared with the value of the undoped sample. The change appears to indicate that some dipoles which are under strong restriction (at the interface) become oriented.

3. Dopant Effect on the Polarization Reversal Process. In order to further understand the dopant effect, it is useful to examine the two sets of data of DPC vs T (Figure 4) and p_y vs T (Figure 5) since they reveal some details of the process of polarization reversal. Figure 6 shows the behavior of DPC and p_y at a fixed temperature after application of a reversal poling

Figure 6

field. Curve (1) is the trace of p_y at 40°C , a part of which is shown in Figure 5 (b). Since p_y is obtained in the cooling cycle after heating up to 140°C , the curve represents the polarization reversal process of the thermally stable dipoles. Curves (2) and (3) are the traces of the depolarization current densities (in Figure 4) at 135°C for doped and undoped samples, respectively. Since the current is measured in a heating cycle, the curves represent the polarization reversal process of the thermally unstable dipoles. The thermally stable dipoles do not reorient if the antiparallel field is lower than about 80 MV/m and suddenly begin to switch around $E_p = 100\text{ MV/m}$ (see curve (1)). This behavior appears to indicate switching of dipoles in the crystalline regions. On the other hand, the thermally unstable dipoles tend to reorient, even if the antiparallel field is lower than 20 MV/m (curves (2) and (3)). This behavior suggests switching of dipoles in the noncrystalline or interface regions. If we define an apparent coercive field, E_c as the intercept of curves (1), (2) and (3) on the E_p axis, they are about 100 , 25 and 55 MV/m , respectively. The enormous decrease in E_c from 55 to 25 MV/m is one of the most prominent dopant effects in the polarization reversal process.

It is interesting to note that the behavior of dipoles with different stability in PVF_2 is also clear in the time domain measurement of the polarization reversal.⁷ The dopant effect shown by the enormous decrease in E_c for the unstable dipoles is also quite consistent with the effect of γ -ray irradiation⁷ on the polarization switching characteristics. Irradiation suppresses the nucleation probability while the presence of

dopant appears to produce exactly the opposite effect. The dopant effect as well as the γ -ray irradiation effect on the polarization reversal process may provide further information about the nucleation and domain growth process in PVF₂ films.

Conclusions

X-ray diffraction data show that the dopant exists outside the crystalline regions of the film; however, even this small amount of TCP (1 wt. %) significantly enhances the low poling field ($E_p \leq 80$ MV/m at room temperature) remnant polarization. The polarization originates from thermally unstable dipole orientation, which is suggestive of their environment: interfacial zones between crystalline and amorphous regions. The TCP also enhances the high poling field ($E_p \geq 120$ MV/m at room temperature) remnant polarization. The polarization originates from thermally stable dipole orientation, which is suggestive of a certain amount of crystal growth at the interfacial zones.

In the polarization reversal process, doping with TCP enormously decreases the coercive field of dipoles which might exist at the nucleation sites of polarization domains, i. e. at the interfacial zones. This may provide further information about the nucleation and growth process during polarization reversal in PVF₂ films.

Acknowledgment. This work was supported by the office of Naval Research.

References and Notes

- (1) Sen, A.; Scheinbeim, J. I.; Newman, B. A. *J. Appl. Phys.* 1984, 56, 2433.
- (2) Kakutani, H. *J. Polym. Sci.* 1970, 8, 1177.
- (3) Murayama, N. *J. Polym. Sci.* 1975, 13, 929.
- (4) Kepler, R. G.; Anderson, R. A. *J. Appl. Phys.* 1978, 49, 1232.
- (5) Scheinbeim, J. I.; Chung, K. T.; Pae, K. D.; Newman, B. A. *J. Appl. Phys.* 1979, 50, 6101.
- (6) Takase, Y.; Tanaka, H.; Wang, T. T.; Caise, T.; Kometani, J. *Macromolecules* 1987, 20, 2318.
- (7) Takase, Y.; Odajima, A.; Wang, T. T. *J. Appl. Phys.* 1986, 60, 2920.
- (8) Wang, T. T. *Ferroelectrics* 1982, 41, 213.
- (9) Furukawa, T.; Date, M.; Fukada, E. *J. Appl. Phys.* 1980, 51, 1135.
- (10) Takahashi, N.; Odajima, A. *Jpn. J. Appl. Phys.* 1981, 20, L59.
- (11) Takase, Y.; Odajima, A. *Jpn. J. Appl. Phys.* 1982, 21, L707.
- (12) Furukawa, T.; Date, M.; Johnson, G. E. *J. Appl. Phys.* 1983, 54, 1540.
- (13) Kaganov, M. I.; Omel'yanchun, A. N. *Soviet Phys. JETP* 1972, 34, 895.
- (14) Binder, K.; Hohenberg, P. C. *Phys. Rev.* 1972, B6, 3461.
- (15) Odajima, A.; Takase, Y.; Ishibashi, T.; Yuasa, K. *Jpn. J. Appl. Phys. Supplement* 1985, 24-2, 881.
- (16) Wada, Y.; Hayakawa, R. *Ferroelectrics* 1981, 32, 115.
- (17) Takahashi, N.; Odajima, A. *Ferroelectrics* 1981, 32, 49.

Figure captions

Figure 1. Diffraction scans (reflection mode) at room temperature of three different samples of uniaxially oriented PVF₂ film; as-received, annealed at 120°C for 2 h, and annealed then immersed in TCP at 100°C for 4 h.

Figure 2. Current densities 2 (a) and electric displacements 2 (b) as a function of electric field when the PVF₂ film is subjected to triangular shape electric field with a period of 1000 s at 20°C. The dotted lines represent data for the doped film and the continuous line for the undoped film.

Figure 3. Depolarization current densities for the doped film 3 (a) and the undoped film 3 (b). Curves (1) - (4) represent the current densities for the films poled by a 1-min step pulse of 20, 60, 120 and 200 MV/m field strength, respectively, and curve (5) poled by sequential step pulses of 200 MV/m strength applied reversely.

Figure 4. Depolarization current densities showing the polarization reversal process of the doped (dotted lines) and the undoped (continuous lines) films. Curves (1) and (2) represent characteristics of the films poled under +200 and -200 MV/m, respectively. Curves (3) and (4) represent characteristics of the film which are subjected to the poling sequence, $E_p = +200$ MV/m, $E_p = -200$ MV/m followed by polarization reversal by applying field of $E_p = +20$ and $+40$ MV/m, respectively. Pulses of the poling field are also shown schematically and each step pulse width is 1 minute.

Figure 5. Pyroelectric coefficients in the cooling cycle after heating up to 140°C of the doped films 5 (a) and of the undoped films 5 (b) as a function of temperature. Curves (1) - (5): poled by a step pulse of 20, 80, 120, 160 and 200 MV/m, respectively. Curve (6): poled by sequential step pulses of +200, -200 and +200 MV/m. Curve (7): poled by a pulse step sequence of +200 MV/m and -200 MV/m. Curve (8): poled by sequential step pulses of +200 MV/m, -200 and +20 MV/m. Curve (9): poled by sequential step pulses of +200 MV/m, -200 and +40 MV/m. Each step pulse width is 1 minute.

Figure 6. Polarization reversal process reflecting switching of thermally stable and unstable dipoles. Curve (1) is the trace of p_y as a function of reversal poling field at 40°C, a part of which is shown in Figure 5 (b). Curves (2) and (3) are the traces of the depolarization current densities as a function of reversal poling field (in Figure 4) at 135 °C for doped and undoped samples, respectively.

Table I

2θ values and half widths, $\beta_{1/2}$, for the (110)(200) reflection for uniaxially oriented phase I PVF₂ films (before poling)

sample	2θ , deg.	$\beta_{1/2}$, deg.
as-received	20.50	1.53
annealed	20.62	1.35
annealed and doped	20.64	1.34

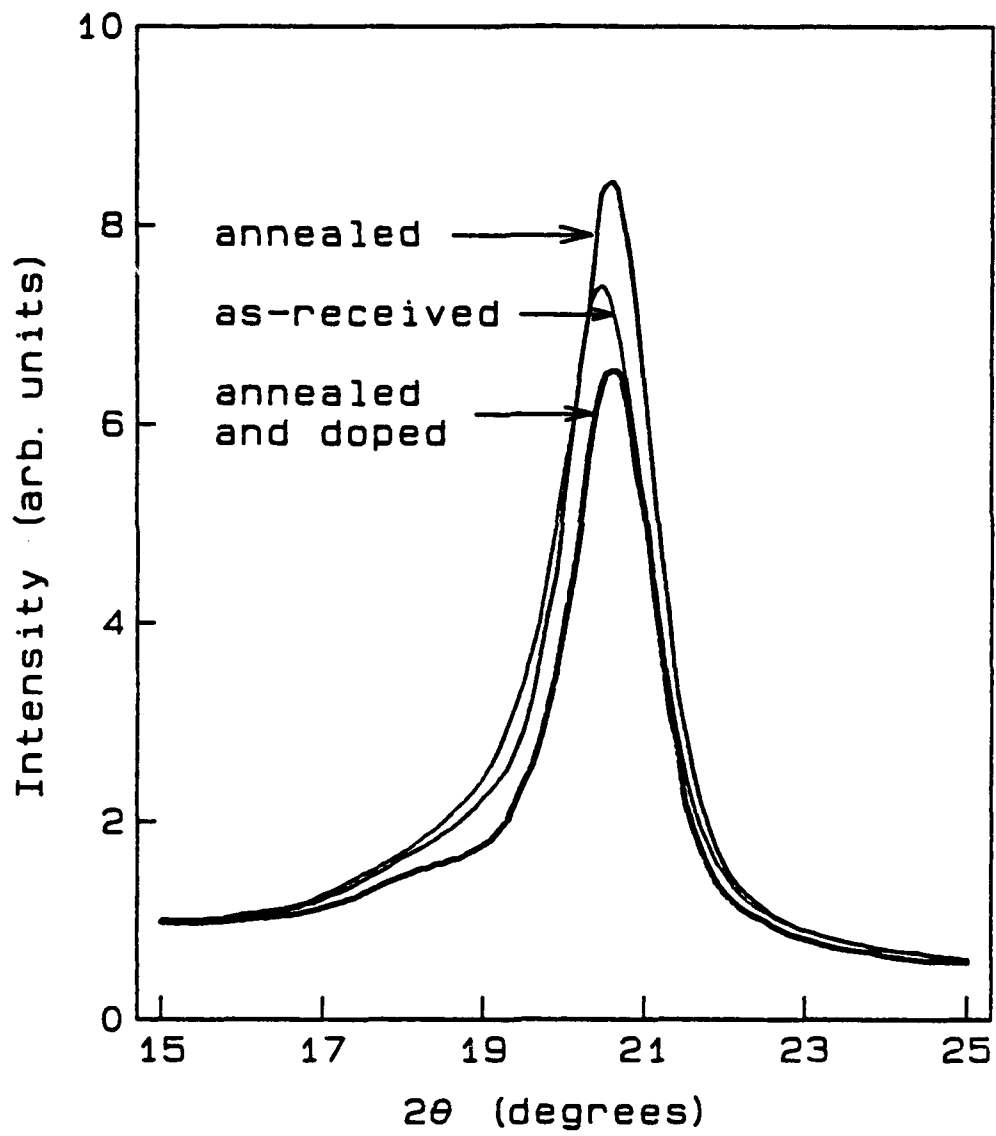


Figure 1.

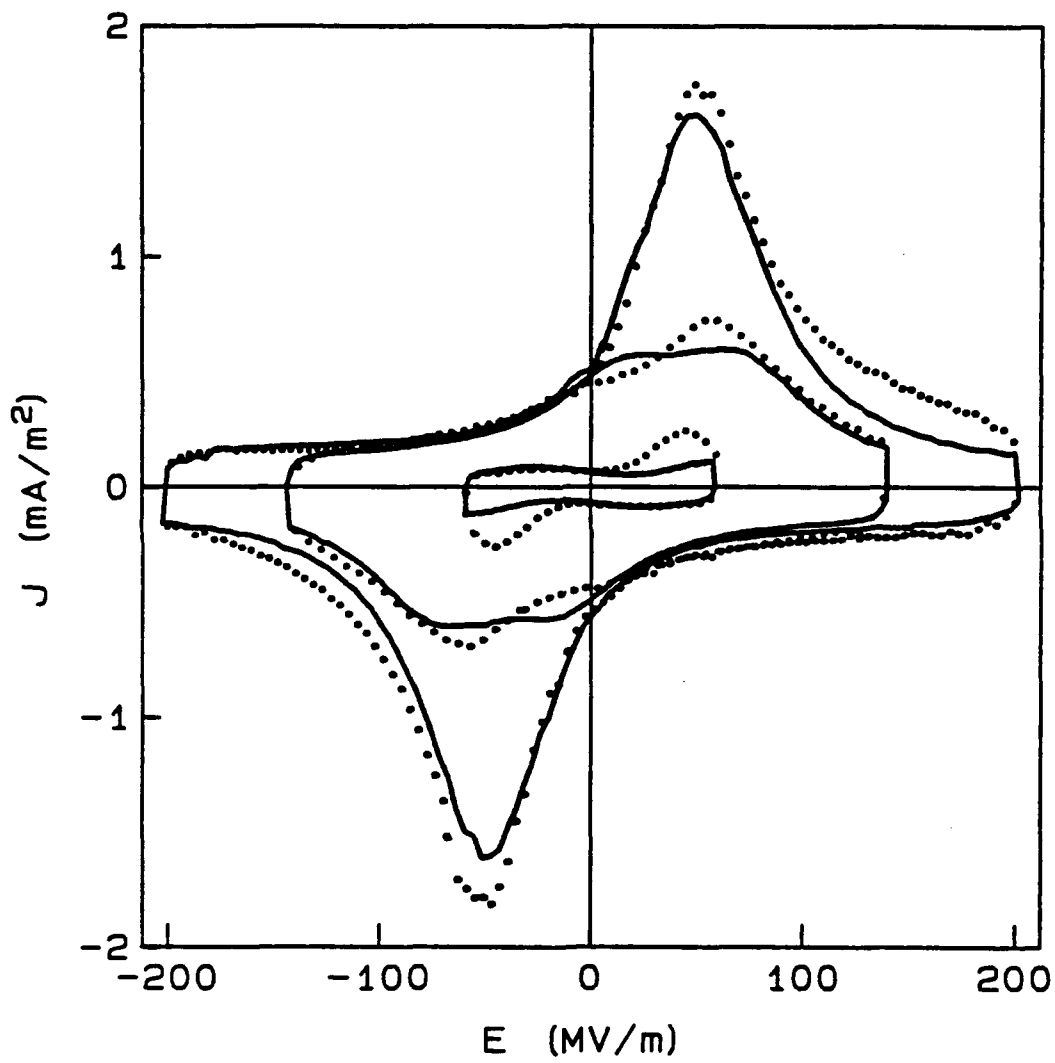


Figure 2 (a).

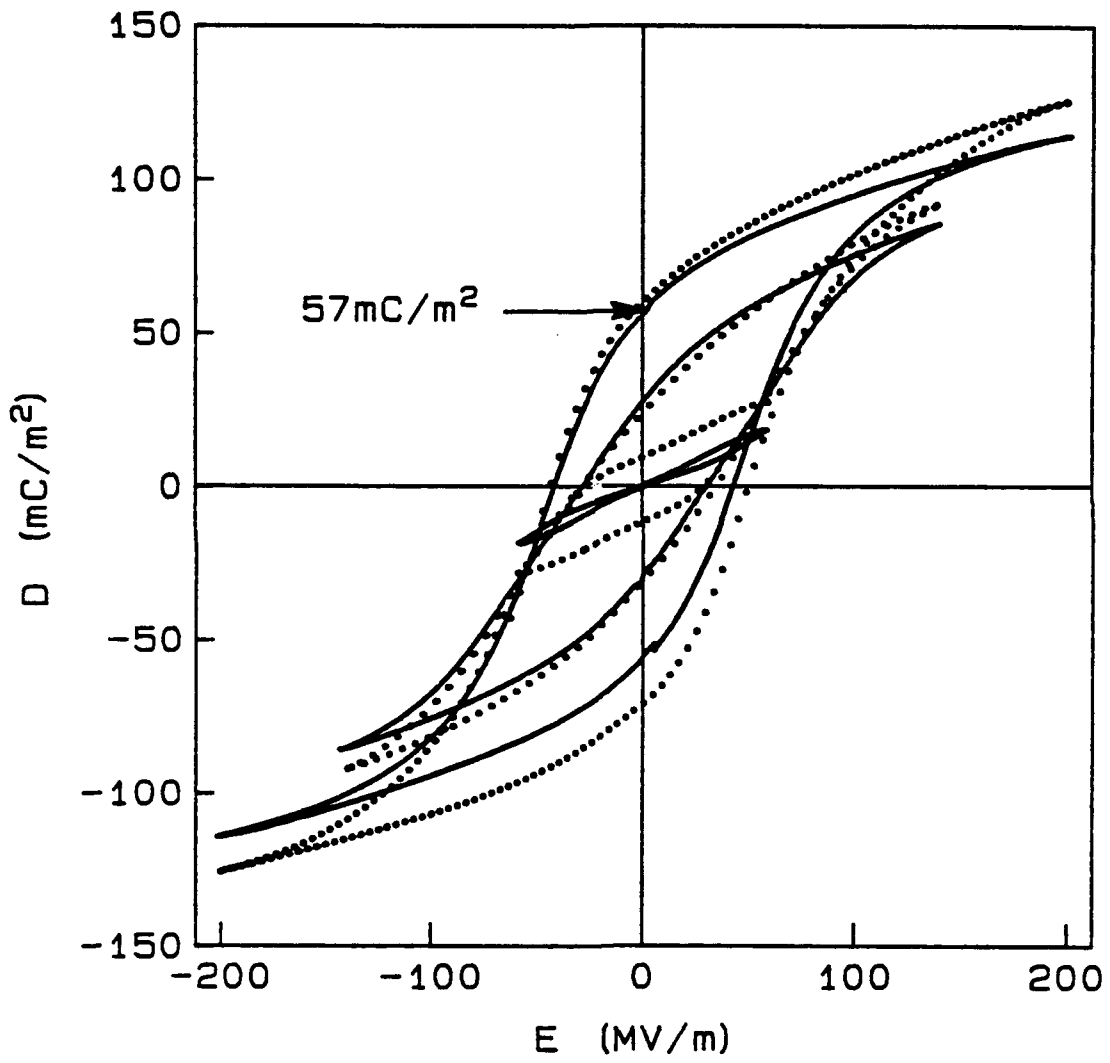


Figure 2 (b).

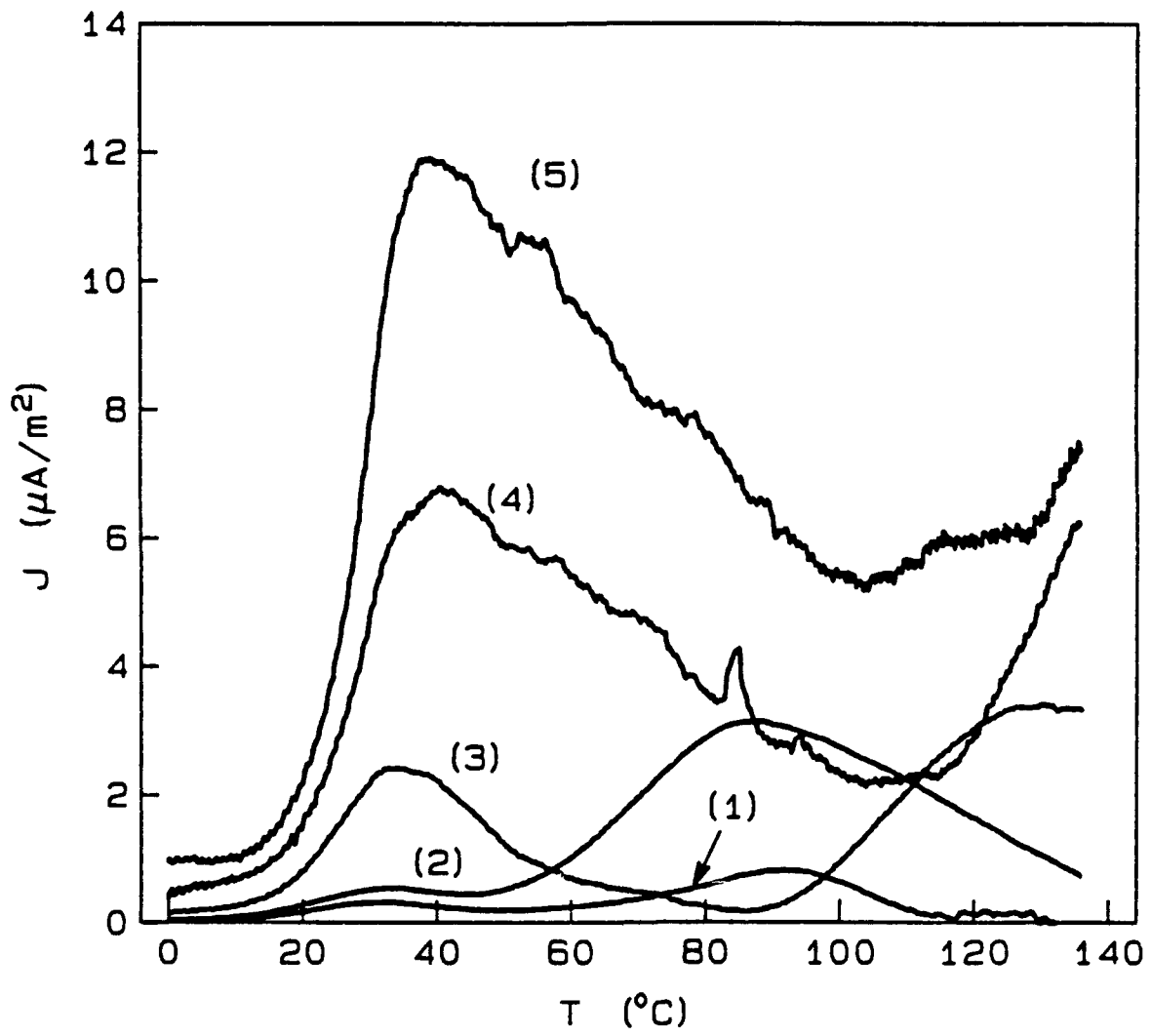


Figure 3(a).

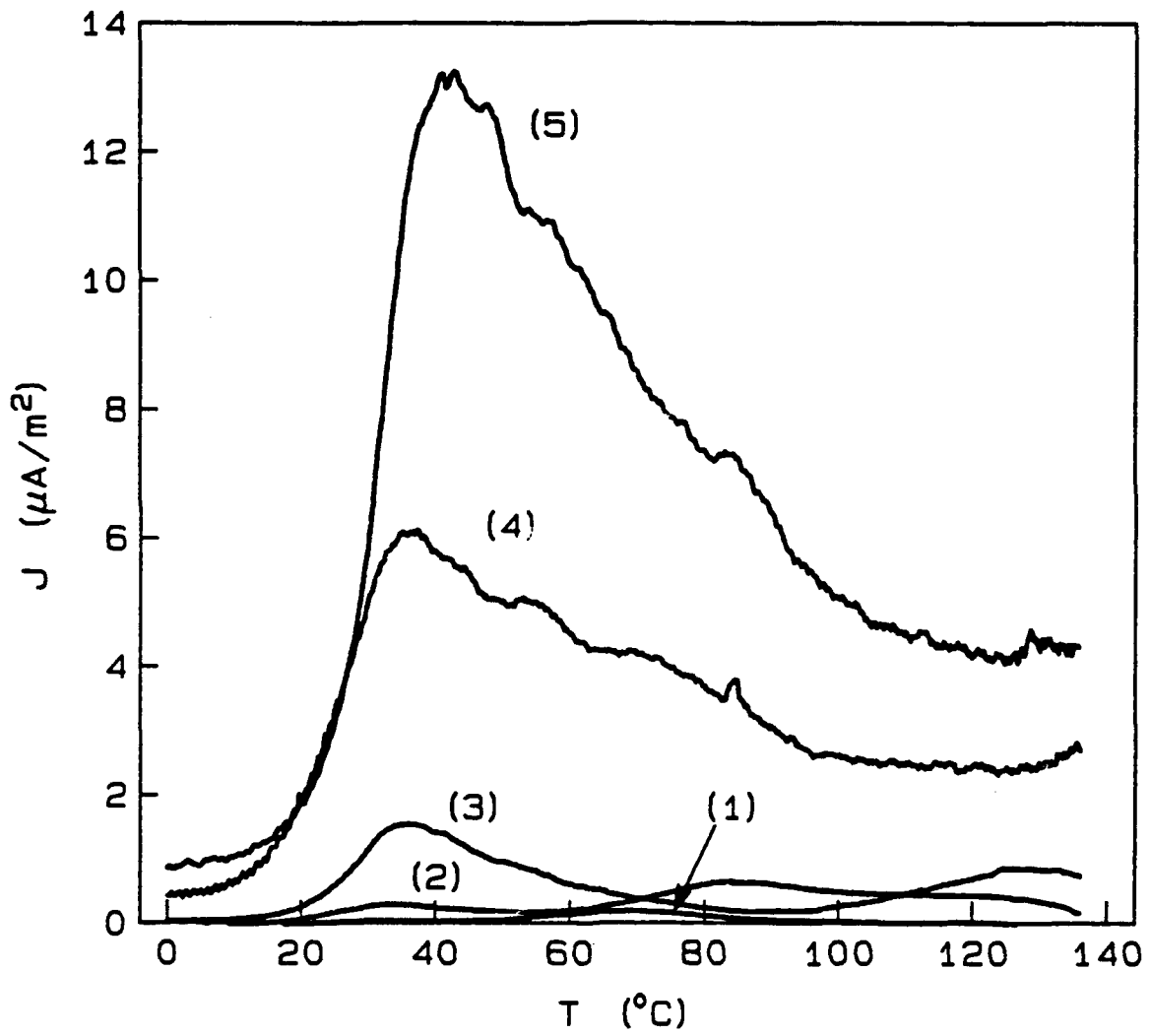


Figure 3 (b).

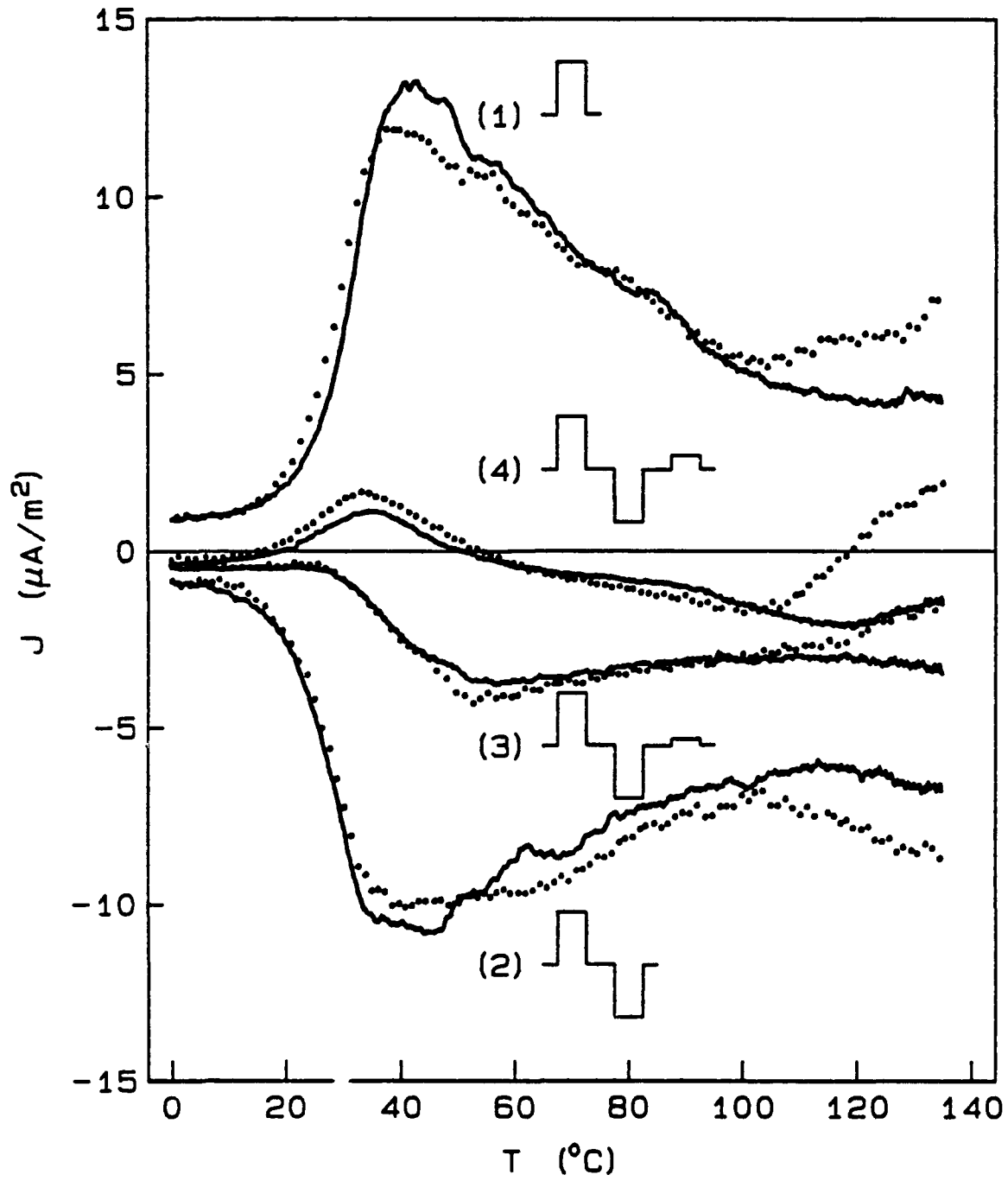


Figure 4.

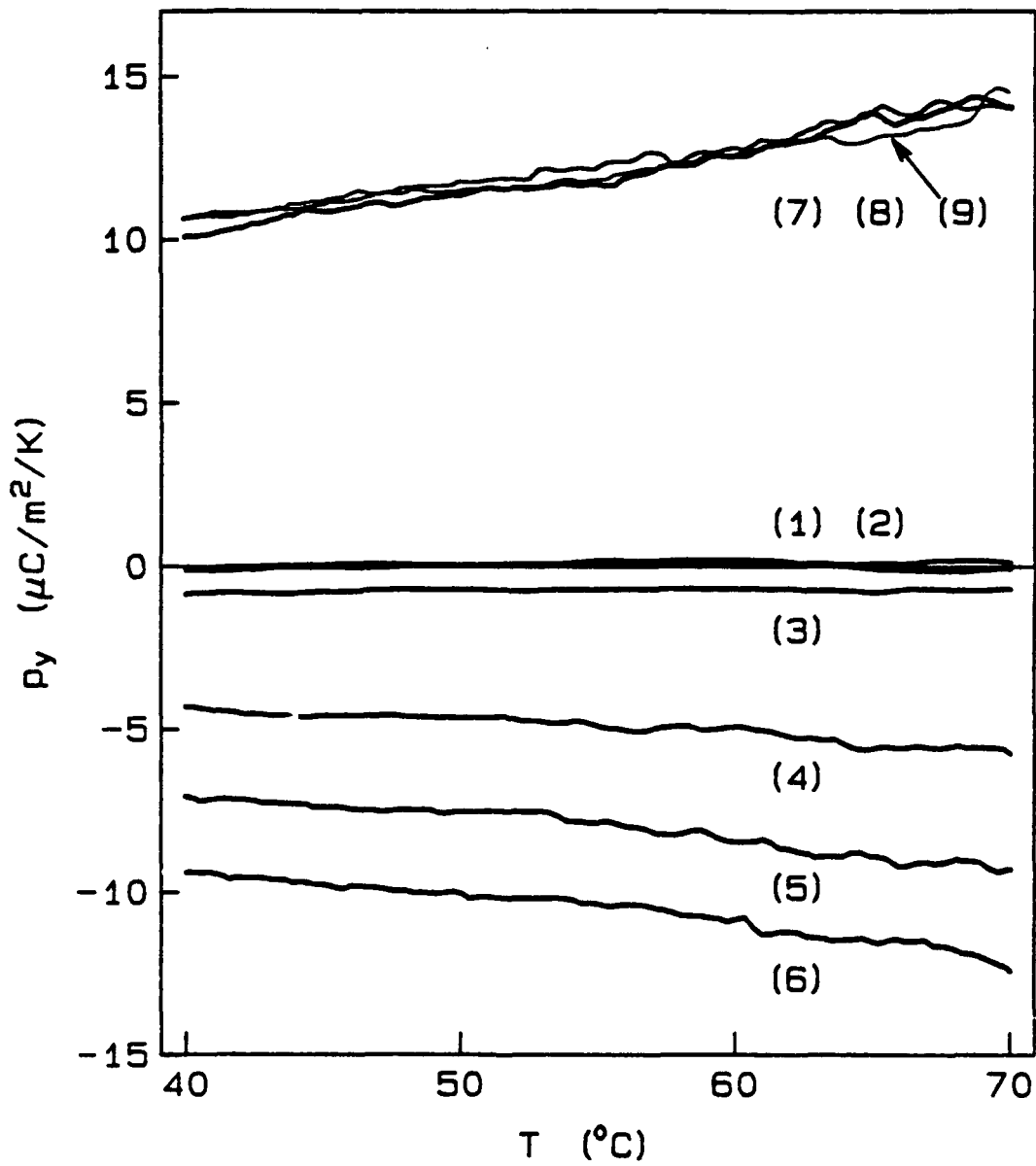


Figure 5(b).

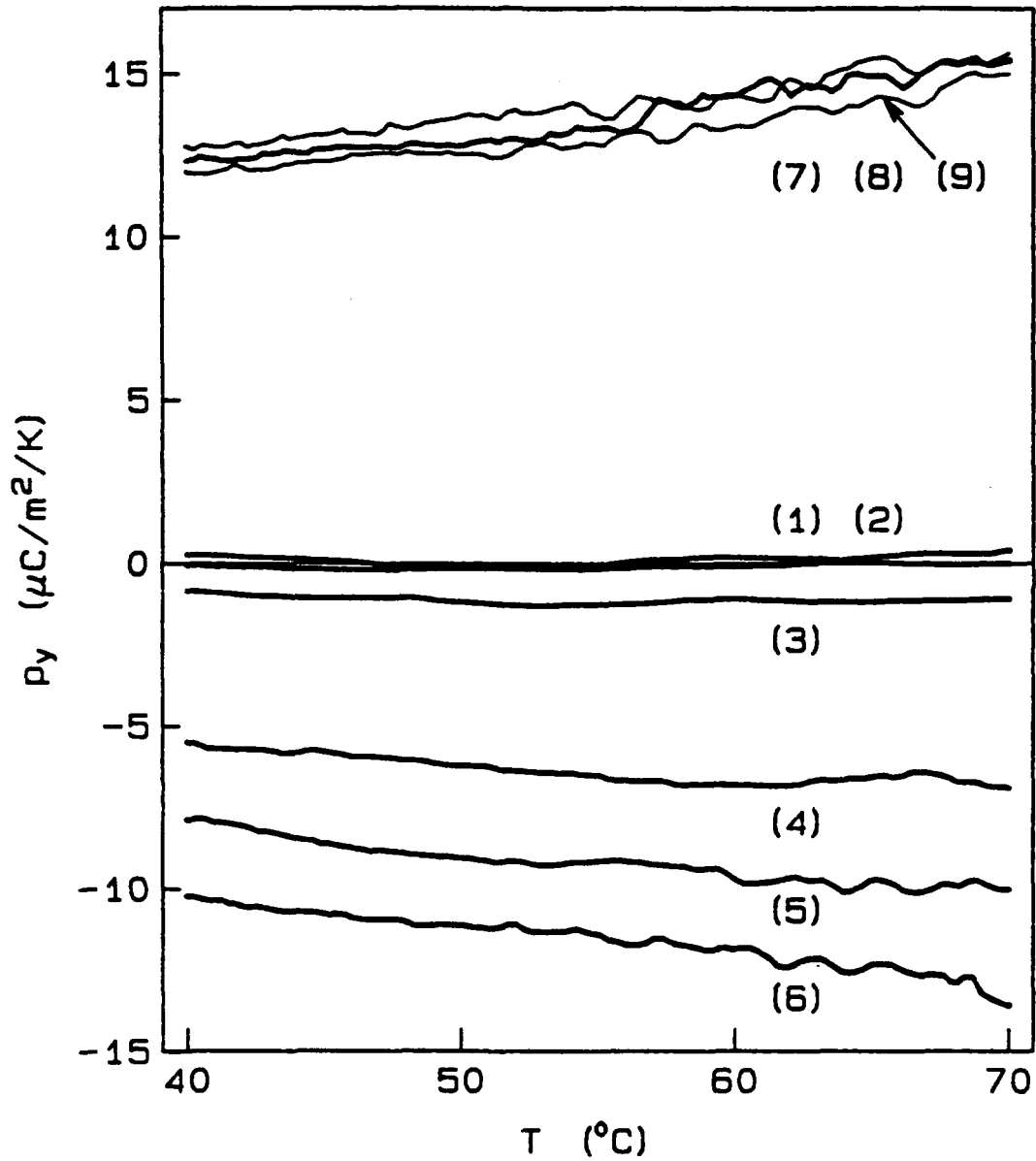


Figure 5(a).

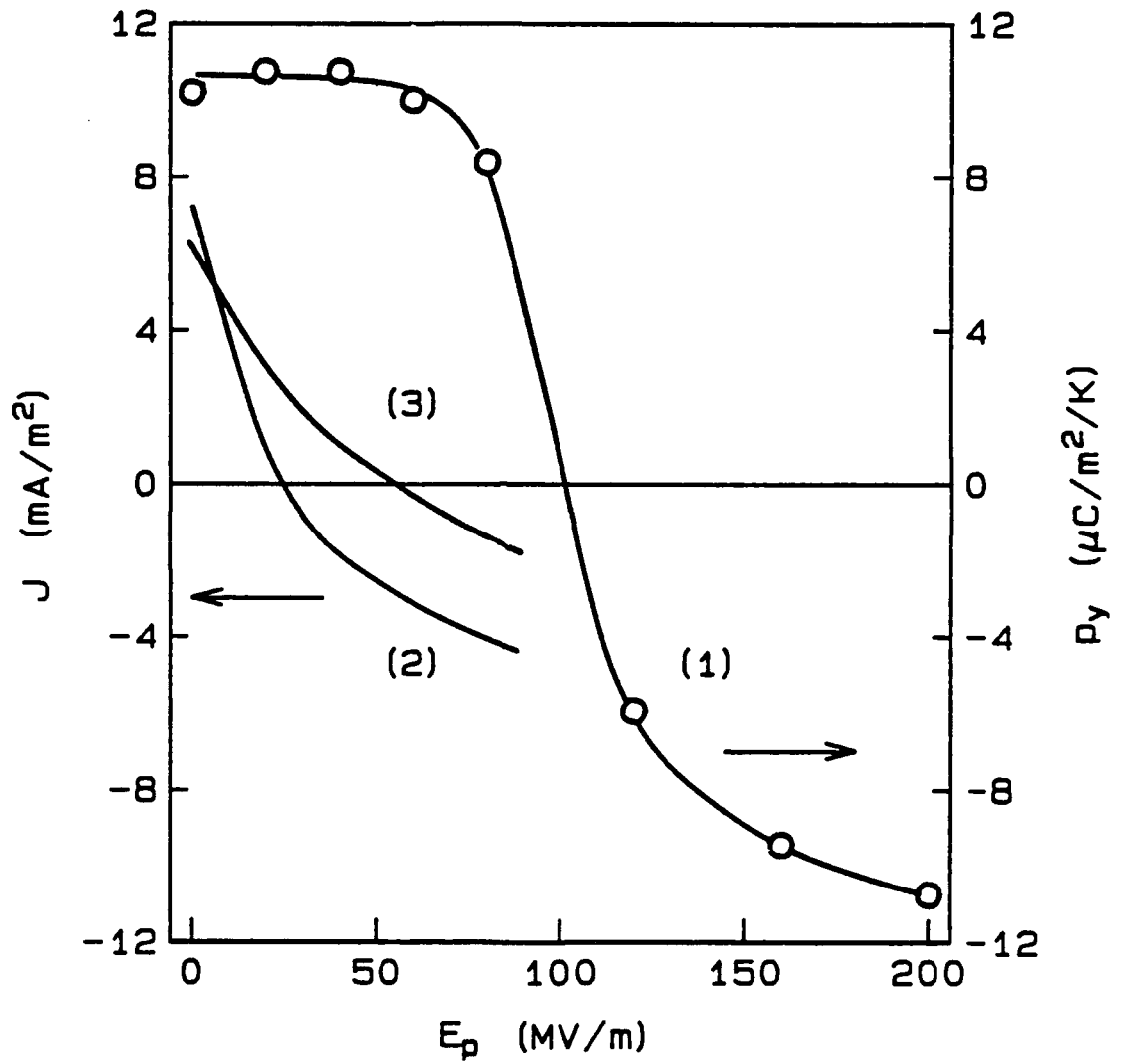


Figure 6.